

# Optical estimation of Gaussian processes without phase reference using Fock states

Changhun Oh,<sup>1,2</sup> Kimin Park,<sup>3,4</sup> Radim Filip,<sup>3</sup> Hyunseok Jeong,<sup>1</sup> and Petr Marek<sup>3</sup>

<sup>1</sup>*Department of Physics and Astronomy, Seoul National University, Seoul 08826, Korea*

<sup>2</sup>*Pritzker School of Molecular Engineering, The University of Chicago, Chicago, Illinois 60637, USA*

<sup>3</sup>*Department of Optics, Palacký University, 17. listopadu 1192/12, 771 46 Olomouc, Czech Republic*

<sup>4</sup>*Center for Macroscopic Quantum States (bigQ),  
Department of Physics, Technical University of Denmark,  
Building 307, Fysikvej, 2800 Kgs. Lyngby, Denmark*

While a general Gaussian process is phase sensitive, a stable phase reference is required to take advantage of this feature. When the reference is missing, either due to volatile nature of the measured sample or technical limitations of the measurement, the resulting process appears as random in phase. Under this condition, there are two single-mode Gaussian processes, displacement and squeezing, and we show that these two can be efficiently estimated using photon number states and photon number resolving detectors. For separate estimation of displacement and squeezing the practical estimation errors for ensembles of hundreds of probes can saturate the Cramér-Rao bound even for arbitrary small values of the estimated parameters and under realistic losses. The estimation of displacement with Fock states always outperforms estimation with the help of Gaussian states with equivalent energy and optimal measurement. For estimation of squeezing Fock states outperform Gaussian methods when their energy is large enough. Finally, we show that Fock states can also be used to estimate the displacement and the squeezing simultaneously.

## I. INTRODUCTION

Quantum metrology with light estimates unknown parameters of quantum processes and reveals the limits of the existing measurements arising from treating the measuring probes as physical systems in specific optimized quantum states [1–4]. In many cases these limits surpass the precision that can be obtained by using probes in classical states, which are those that can be described without use of quantum optics. Typical examples can be found in optical interferometry [5], where the precision of measuring phase can be improved by using squeezed states of light [6–9], or elaborately constructed superpositions of individual photons [10–12]. A specific case of optical interferometry relies on homodyne detection [13], where the reference arm of the interferometer is represented by a classical local oscillator beam [7–9], which leaves only the probe to be prepared in a quantum states. It was shown that even in this semi-single mode scenario, nonclassical quantum states can be used to enhance measurement of phase [7–9] and displacement [14–16].

However, while the nonclassical quantum states have been shown to significantly outperform the classical methods in ideal cases [7, 10], they are highly vulnerable to experimental imperfections. In Gaussian scenarios [9, 14, 17–22], such as employing squeezed states to boost interferometry, the losses of the quantum state simply reduce its effectiveness [8, 9]. In non-Gaussian cases, such as employing so-called NOON states used for estimation of phase, losses can completely remove the quantum advantage [12, 23], while recent progress tries to alleviate this effect [24].

A significant source of imperfections in optical interferometry is the fluctuation of phase in the measured sample. It is particularly hindering to the estimation of phase sensitive processes, such as Gaussian displacement and squeezing, or to any strategies employing phase sensitive resources, such as squeezed states and homodyne detection. Keeping the phase steady requires active stabilization inside the sample which may not always be feasible. However, control of the phase is not necessary for estimating strength of the phase sensitive operations. This was shown in a recent trapped ion experiment [25], where the size of displacement, a generally phase sensitive operation, was estimated without any kind of phase reference, just relying on Fock state preparation and measurement.

In this paper we show that optical estimation of the strength of Gaussian operations, displacement and squeezing, can be indeed realized without any phase reference with Fock states and measurements in photon number basis. For the case of displacement, this approach surpasses even optimal Gaussian methods, which are based on homodyne detection and squeezed states with equivalent energy and which use the phase reference. In the case of squeezing estimation, Fock states are generally comparable to Gaussian methods at weak energies, overcoming them for larger energies of the probe states. Our probe states do not need to be pure and can have advantage over the Gaussian probe states even for realistic losses of the order of 20%. Finally we show that this approach can be useful for simultaneous estimation of both quantities [26].

## II. GENERAL MODEL

In our quantum sensing protocol for Gaussian processes without a stable phase, represented by a superposition of quantum evolution with all phases, we start with an ensemble of  $M$  probes prepared in a well-defined quantum state that is fully under our control. The probes then sequentially interact with a sample, undergoing weak phase randomized Gaussian evolution in the process, and are measured by a specific measurement. The measured data are then evaluated with the help of maximum likelihood estimator (MLE) to extract the unknown parameters of the Gaussian operation. In our analysis we will focus on photon number resolving detectors (PNRD).

In the absence of stable phase in the sample, the general Gaussian evolution of the probe state  $\hat{\rho}_{in}$  can be represented by a completely positive trace preserving map  $\mathcal{M}$ :

$$\hat{\rho}_f(N_c, N_s) = \mathcal{M}(\hat{\rho}_{in}) = \int_0^{2\pi} \frac{d\phi_1}{2\pi} \int_0^{2\pi} \frac{d\phi_2}{2\pi} \hat{D}(\sqrt{N_c}e^{i\phi_1}) \hat{S}(\sqrt{N_s}e^{i\phi_2}) \hat{\rho}_{in} \hat{S}^\dagger(\sqrt{N_s}e^{i\phi_2}) \hat{D}^\dagger(\sqrt{N_c}e^{i\phi_1}), \quad (1)$$

where  $\hat{D}(\alpha) = \exp(\alpha\hat{a}^\dagger - \alpha^*\hat{a})$  and  $\hat{S}(\xi) = \exp[(\xi\hat{a}^{\dagger 2} - \xi^*\hat{a}^2)/2]$  represent the unitary Gaussian displacement and squeezing operations, respectively. However, it should be noted that, due to the phase randomization, the overall operation is neither unitary, nor Gaussian. In contrast to general pure Gaussian unitary with five parameters, the phase indeterminate operation has only two free parameters:  $N_c$  related to the average linearized energy added by the displacement, and  $N_s$  related to the energy added by the squeezing. On vacuum state  $\hat{\rho}_{in} = |0\rangle\langle 0|$ , the added energies of the two operations are given as  $N_c$  for displacement and  $\sinh^2(\sqrt{N_s})$  for squeezing. In the limit of weak strengths  $N_s$  and  $N_c$ , which is the regime we are interested in, phase insensitive displacement and squeezing operations commute and the average photon number is increased by  $N_s + N_c$ .

Before we proceed, let us establish some theoretical framework by briefly recalling the quantum Cramér-Rao (QCR) inequality and the quantum Fisher information (FI). QCR inequality states that for a given probe and channel that encodes an unknown parameter of interest  $\theta$ , the estimation error of any unbiased estimator is bounded by the inverse of quantum FI [27, 28],

$$\Delta^2\theta \geq \frac{1}{MH(\theta)}, \quad (2)$$

where the variance  $\Delta^2\theta = \langle(\theta^{\text{est}} - \theta)^2\rangle$  is the estimation error, and  $M$  is the number of trials in an experiment, and  $H(\theta) = \text{Tr}(\hat{\rho}_\theta \hat{L}_\theta^2)$  is the FI of the probe state after the encoding. It is known that the lower bound is asymptotically saturable by using MLE [29–31]. In experiments, the optimal precision suggested by equality in (2) is obtained by an optimal positive operator valued measurement (POVM), which can be found by the eigenbasis of the symmetric logarithmic derivative operator  $\hat{L}_\theta$  satisfying an equation,

$$\frac{\partial \hat{\rho}_f}{\partial \theta} = \frac{\hat{\rho}_f \hat{L}_\theta + \hat{L}_\theta \hat{\rho}_f}{2}. \quad (3)$$

If the density matrix of the output state is diagonalized as  $\hat{\rho}_\theta = \sum_n \rho_n |\psi_n\rangle\langle\psi_n|$ , the symmetric logarithmic derivative operator is given  $\hat{L}_\theta = 2 \sum_{n,m} \frac{\langle\psi_n|\partial_\theta \hat{\rho}_f|\psi_m\rangle}{\rho_n + \rho_m} |\psi_n\rangle\langle\psi_m|$  [32]. When the optimal measurement is chosen, the classical FI

$$F(\theta) = \sum_n \frac{1}{p(n|\theta)} \left( \frac{\partial p(n|\theta)}{\partial \theta} \right)^2 \quad (4)$$

becomes the quantum FI where  $p(n|\theta) = \text{Tr}(\hat{\rho}_f \hat{\Pi}_n)$  with  $\{\hat{\Pi}_n\}$  being an optimal POVM, i.e. the projectors of eigenstates of  $\hat{L}_\theta$ . According to QCR inequality (2), FI lower-bounds the estimation error obtainable during the actual measurement by  $\Delta^2 N_c = 1/MF$  where  $M$  is the number of trials. In a general scenario, however, there is no guarantee that this bound can be achieved with a practical number of  $M$  although it is achievable using the MLE in an asymptotic regime of  $M \rightarrow \infty$ . In the following sections, we present the estimation error of our scenario obtained by the MLE for a finite number of  $M$ .

Map (1) is phase insensitive; it commutes with any phase shift applied to the state of the probe. Consequently, if the probe state is phase insensitive it remains so. This suggests that a well-defined phase of the probe may not be required for optimal estimation. This can be illustrated on an example of probe prepared in Fock state  $\hat{\rho}_{in} = |m\rangle\langle m|$ . Such probe is pure but completely phase insensitive. In the limit of weak strengths  $N_c, N_s \ll 1$ , map (1) transforms

the initial pure state of the probe into a mixture of Fock states with weights as:

$$p(m-2|N_c, N_s) \simeq N_s m(m-1)/4 \quad (5)$$

$$p(m-1|N_c, N_s) \simeq N_c m \quad (6)$$

$$p(m|N_c, N_s) \simeq 1 - N_c(2m+1) - N_s(m^2 + m + 1)/2 \quad (7)$$

$$p(m+1|N_c, N_s) \simeq N_c(m+1) \quad (8)$$

$$p(m+2|N_c, N_s) \simeq N_s(m+2)(m+1)/4. \quad (9)$$

Since the state is diagonal in the Fock basis these weights can be perfectly measured by PNRD. In this important limit we can see that the displacement and squeezing unitaries act in a complementary way - displacement changes the photon number by one, squeezing changes it by two. This indicates that in this limit the two operations can be discerned independently.

The measured data, with the help of Eqs. (5)-(9), can be used to construct MLEs for each parameter. Let us denote the number of outcomes corresponding to detecting particular state  $|k\rangle$  by  $n_k$  with  $k \in \{m-2, m-1, m, m+1, m+2\}$ ; thus,  $\sum_{k=m-2}^{m+2} n_k = M$ , where  $M$  is again the total number of trials. We simply ignore the outcome out of the above range since the probability is negligible for very small strength of the signal. By maximizing the log-likelihood function  $\log L(\mathbb{D} = \{n_k\}|N_c, N_s) = \sum_k n_k \log p(k|N_c, N_s)$  for each parameter  $N_c$  and  $N_s$ , one can find that the MLE is written as

$$N_c^{\text{est}} = \frac{n_{m-1} + n_{m+1}}{M(2m+1)}, \quad \text{and} \quad N_s^{\text{est}} = \frac{2(n_{m-2} + n_{m+2})}{M(m^2 + m + 1)}, \quad (10)$$

and that they are unbiased for any  $M > 0$ , i.e.,  $\langle N_c^{\text{est}} \rangle = N_c$  and  $\langle N_s^{\text{est}} \rangle = N_s$ , where the bracket represents the average over all possible outcomes. The form of the MLEs, in particular the exclusive use of the respective count numbers  $n_k$ , implies that each parameter can be estimated simultaneously without knowing the other parameter.

In addition, from the same equations we can derive classical FI to evaluate the estimation of  $N_c$  and  $N_s$  by using a PNRD, which we can then compared to the upper limit given by quantum FI for the optimal detector. For the case of phase insensitive states, PNRD gives us full available information and the classical FI is equal to quantum FI. Based on Eqs. (5)-(9), the classical FI of Fock states can be approximately found to be:

$$F(N_c) \approx \frac{2m+1}{N_c}, \quad (11)$$

for displacement and

$$F(N_s) \approx \frac{m^2 + m + 1}{2N_s}, \quad (12)$$

for squeezing in the limit of  $N_c, N_s \ll 1$ . In this limit, one can derive the average estimation error of ML estimators (10)

$$\Delta^2 N_c \approx \frac{N_c}{M(2m+1)} \quad \text{and} \quad \Delta^2 N_s \approx \frac{2N_s}{M(m^2 + m + 1)}, \quad (13)$$

which is consistent with the FI. For both of them the performance improves with the increased Fock number of the probe, linearly in the case of displacement while quadratically in the case of the squeezing. Both quantities diverge as the signal decreases, but the relative estimation errors, which are given as inverse of the Fisher information relative to the signal,  $R = \frac{1}{F(N_i)N_i}$  with  $i = c, s$ , attain constant value. In the next sections, we will analyze how these values can be obtained with a realistic number of probes and how is the procedure affected by realistic processing and imperfections in comparison to results obtainable with Gaussian resources.

### III. DISPLACEMENT ESTIMATION WITH FOCK STATE PROBE

Let us first analyze situations in which the displacement operation is the only relevant effect. In this case, the operation is represented by map (1) with the squeezing parameter  $N_s = 0$ . It transforms the initial Fock state  $|m\rangle\langle m|$  into a mixed state

$$\hat{\rho}_f(N_c) = \int_0^{2\pi} \frac{d\phi}{2\pi} \hat{D}(\sqrt{N_c}e^{i\phi})|m\rangle\langle m|\hat{D}^\dagger(\sqrt{N_c}e^{i\phi}) = \sum_{n=0}^{\infty} p(n|N_c)|n\rangle\langle n|, \quad (14)$$

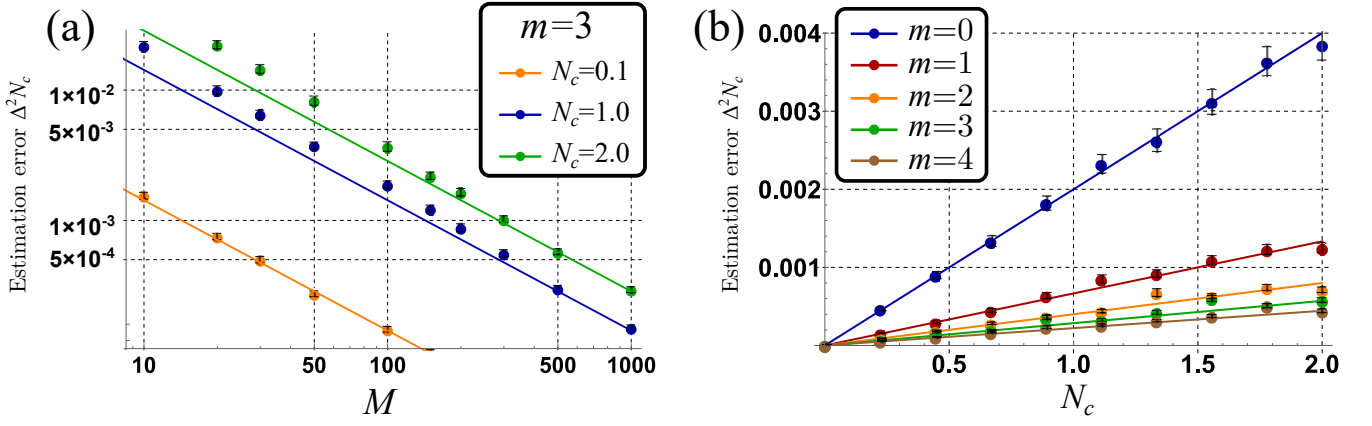


FIG. 1. Simulation for displacement estimation error  $\Delta^2 N_c$ . (a) Against the number of copies  $M$  for various strengths  $N_c = 0.1, 1.0, 2.0$  by a Fock state probe  $|m = 3\rangle$ . Lines and dots represent the inverse of FI (CR bound) and the estimation errors of simulations averaged over 3000 trials using MLE. (b) Against the signal energy  $N_c$  for various input probe Fock number  $m = 0, 1, 2, 3, 4$  with the number of copies  $M = 500$ . Again the lines and dots are inverse of FI and errors obtained by simulation averaged over 3000 trials using MLE. Throughout the paper, error bars represent twice the standard deviation of the obtained estimation error divided by the square root of the number of simulation runs.

where

$$p(n|N_c) = |\langle n|\hat{D}(\sqrt{N_c})|m\rangle|^2 = \frac{m!}{n!} e^{-N_c} N_c^{n-m} L_m^{(n-m)}(N_c)^2, \quad (15)$$

is the conditional probability to detect  $n$  photons for a given  $N_c$  and  $m$  with  $L_m^n(x)$  being associated Laguerre polynomials [33]. Since the final state is diagonal in Fock basis, it has equal quantum and classical FI for PNRD:

$$F(N_c) = \sum_{n=0}^{\infty} \frac{1}{p(n|N_c)} \left( \frac{\partial p(n|N_c)}{\partial N_c} \right)^2 = \frac{2m+1}{N_c}, \quad (16)$$

which is exactly the value approached by the approximate relation (11). It implies that in the limit of weak strength  $N_c \ll 1$ , the protocol of the MLE of Eq. (10) is the optimal procedure. The derivation of the FI is supplied in Appendix A. It should be noted that the monotonous increase of FI with the energy of the state  $m$  requires the measurement in the Fock basis. If the measurement was replaced by measurement of the mean energy  $\langle \hat{n} \rangle$ , the size of displacement could still be inferred, but the error of the measurement increases with  $m$  (see Appendix B for detail).

To see whether practical errors can reach the bounds given by classical FI, we have performed a numerical simulation of the full protocol of estimating displacement with Fock state probes and PNRD. For each scenario given by a different combination of  $m$  and  $N_c$ , we have generated 3000 sets of simulated data  $\mathbb{D}$  with probability distributions  $p(n|N_c)$  and evaluated them with a MLE,  $N_c^{\text{est}}$ , obtained by numerical maximization over a finite range, corresponding to a prior knowledge, of the log-likelihood function:

$$\log L(\mathbb{D} \equiv \{n_k\}|N_c) = \sum_{k=0}^{\infty} n_k \log p(k|N_c), \quad (17)$$

where  $n_k$  is the number of outcomes for  $k$  photons. The estimated value  $N_c^{\text{est}}$  was then compared to the true value  $N_c$  to obtain the estimation error  $\Delta^2 N_c = \langle (N_c^{\text{est}} - N_c)^2 \rangle$  and compared to the QCR bound. The results of the simulations can be seen in Fig. 1, where the simulated runs, marked by points, are compared to the bounds derived from quantum FI, represented by lines. In Fig. 1a we can see that, for probe in state  $|3\rangle$ , the realistic estimation error shows the same scaling as the bounds given by FI, saturates this bound already for  $M = 500$  and that this scaling does not depend on the estimated value. Both the dependence on  $M$  and  $N_c$  show that the the QCR bound is practically achievable with a finite  $M$ . Fig. 1b then confirms that this behavior holds even for probes prepared in different Fock states. It is worth noting that when the signal strength is small  $N_c \ll 1$ , the process becomes a binary outcome estimation problem of  $n_{m-1} + n_{m+1}$  and  $n_m$  in Eq. (10) so that the CR inequality is saturated by the ML estimator for any number of copies  $M$  as shown in (13).

Since quantum FI for Fock state probes is achievable by estimation with PNRD, we can use it for further analysis. For comparison we can consider practical Gaussian estimation methods employing Gaussian probes and stable phase

between the input and the measured state. Even though the operation is random in phase, the stable phase is actually the most optimistic scenario for the Gaussian tools, because it enables noise reduction coming from squeezed vacuum fluctuations [34]. If we lifted this assumptions and considered phase randomized Gaussian states or, equivalently, Gaussian states with phase randomized detection, their performance would be necessarily worse than that of Fock states. For our comparison we shall therefore consider quantum FI of phase sensitive Gaussian states which might be higher than what can be achievable by Gaussian measurements. In this way we are comparing realistic estimation based on Fock states with the upper bound for Gaussian states.

Let us denote the output state from a channel with a parameter  $\theta$  as  $\hat{\rho}_\theta$ . In our case, the unknown parameter  $\theta$  corresponds to the amount of energy  $N_c$  pumped by the displacement. The quantum FI of these density matrix can be found [28]:

$$H(\theta) = \frac{4[1 - \mathcal{F}(\hat{\rho}_\theta, \hat{\rho}_{\theta+d\theta})]}{d\theta^2}, \quad (18)$$

where  $\mathcal{F}(\hat{\rho}_0, \hat{\rho}_1) = \left( \text{Tr} \sqrt{\hat{\rho}_0^{1/2} \hat{\rho}_1 \hat{\rho}_0^{1/2}} \right)^2$  is the quantum fidelity between two quantum states  $\hat{\rho}_0$  and  $\hat{\rho}_1$ . Any Gaussian probe in a pure state can be expressed as a displaced squeezed vacuum state  $\hat{D}(\beta)\hat{S}(\zeta)|0\rangle$ . Finding the optimal Gaussian probe requires maximization of the FI over the two parameters  $\beta$  and  $\zeta$  under the chosen constraints such as the total mean photon number in the input state. One can easily check that the value of  $\beta$  does not change the precision; thus, the optimal Gaussian probe is a squeezed state without any displacement possessing the lowest energy. In Fig. 2 we show the comparison of classical FI for Fock probes with PNRD, marked by dots, quantum FI of optimized Gaussian probes with equal energy, marked by solid lines, and quantum FI for vacuum state, marked by dashed lines, for the estimation of the unknown phase-insensitive displacement operations with various  $N_c$ . We can see that the Fock state probes are superior to optimal Gaussian probes with the same mean photon number for the entire range of displacement strengths even though the former requires no phase stability and the latter may use arbitrary coherent detection schemes. This improvement is most prominent for large values  $N_c$ . Note that since quantum FI is used to assess the achievable estimation precision of Gaussian states, and the final state from a squeezed state probe is generally phase-sensitive, we are implicitly assuming that a stable reference beam outside of the sensor is prepared and may be properly used for phase-sensitive measurement. Without this reference the state needs to be treated as phase randomized squeezed state, which always performs worse than Fock state with equivalent energy, and is even definitely inferior to the vacuum state for low energies.

Let us now discuss the effects of optical imperfections, such as losses, to ensure the validity of the results in practical scenarios. The photon-loss process, which is the main imperfection for light, can be described by quantum master equation in the interaction picture as [35]

$$\frac{d\hat{\rho}}{dt} = \frac{\gamma}{2} (2\hat{a}\hat{\rho}\hat{a}^\dagger - \hat{\rho}\hat{a}^\dagger\hat{a} - \hat{a}^\dagger\hat{a}\hat{\rho}), \quad (19)$$

where  $\gamma$  is the loss parameter. The loss rate is defined as  $1 - \eta = 1 - e^{-\gamma t}$  with  $t \geq 0$  describing the monotonous decay of the coherence terms. This dynamics can be equivalently described with a virtual beam splitter interaction

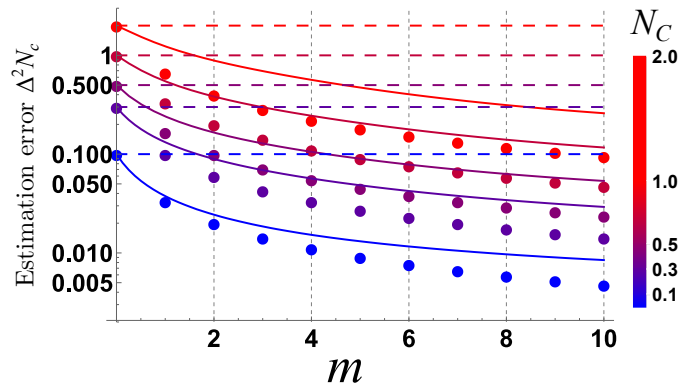


FIG. 2. Comparison between the lower bounds on estimation error given by the inverse of classical FI of Fock states with PNRD (dots), quantum FI of squeezed states with mean photon number equal to  $m$  (solid lines), and quantum FI of coherent states (dashed lines) with mean photon number equal to  $m$ . Quantum FI for squeezed states was calculated numerically. Different colors correspond to different values of the estimated parameter,  $N_c = 0.1, 0.3, 0.5, 1.0, 2.0$ , and are specified by the color bar. The squeezing required for energies equivalent to  $m = 2, 4, 6, 8, 10$  amounts to 10.0, 12.5, 14.1, 15.3, 16.2 dB.

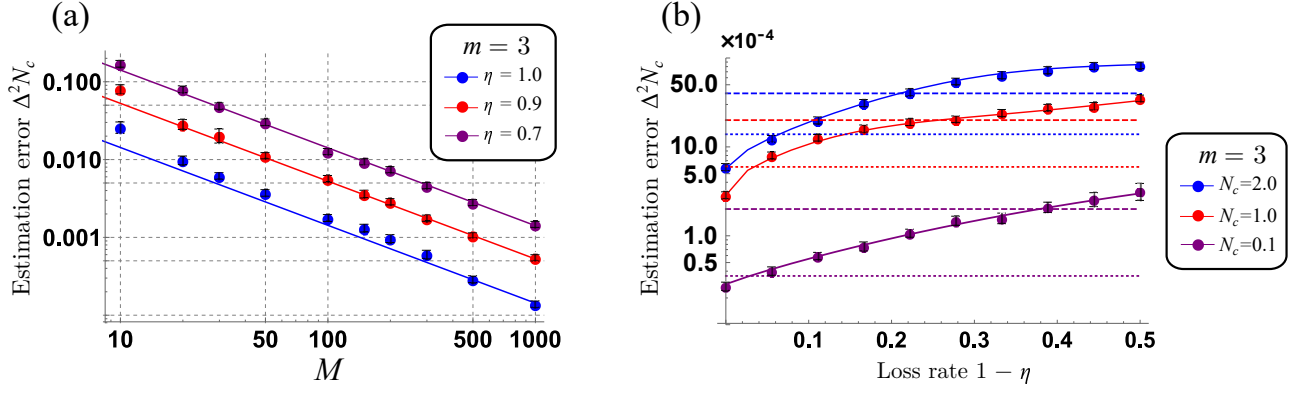


FIG. 3. Simulation for displacement estimation in the presence of photon-loss before the sample. Dots and solid lines represent estimation errors and inverse quantum FI. (a) Against the number of copies  $M$  for different loss rates,  $\eta = 1, 0.9, 0.7$  for  $N_c = 1.0$  and  $|m = 3\rangle$ . (b) Against the loss rate  $1 - \eta$  for different values of the measured displacement  $N_c = 0.1, 1.0, 2.0$  with input probe  $|m = 3\rangle$  and  $M = 500$ . Classical limits (dashed lines) given by coherent states, and optimal Gaussian limits (dotted lines) by squeezed state with the same energy are evaluated from the inverse quantum FI without the losses.

coupling the probe with a zero temperature bath. The losses can manifest either before the sample and thus represent the degradation of the probe, or after the sample and be related to imperfection of the measurement. In the case of displacement estimation, the two losses act in almost the exactly the same way, only the one after the channel also reduces the measured quantity. To be more exact, if we represent the losses by completely positive trace-preserving map [23]

$$\mathcal{L}_\eta(\hat{\rho}) = \sum_{k=0}^{\infty} \hat{A}_k \hat{\rho} \hat{A}_k^\dagger, \quad \hat{A}_k = \frac{\sqrt{1-\eta}^k}{\sqrt{k!}} \sqrt{\eta} \hat{a}^\dagger \hat{a}^k, \quad (20)$$

then the losses after the displacing sample and before the displacing sample can be related as  $\mathcal{L}_\eta[\hat{D}(\sqrt{N_c})\hat{\rho}_{in}\hat{D}^\dagger(\sqrt{N_c})] = \hat{D}(\sqrt{\eta N_c})\mathcal{L}_\eta(\hat{\rho}_{in})\hat{D}^\dagger(\sqrt{\eta N_c})$ . We can see that the losses affect the probe in exactly the same way and the only difference is in scaling of the estimated parameter. Displacement adding energy  $N_c$  before the loss is equivalent to displacement adding energy  $\eta N_c$  after the loss. In addition, this behavior remains also for the Gaussian states. For the sake of simplicity we can therefore consider only the losses before the sample. It should be noted that we assume  $\eta$  is known through prior measurements and not a subject of the estimation.

In numerical simulation shown in Fig. 3, the theoretical Fock state distribution  $p(n|N_c, \eta)$  was used to generate 1000 sets of data, which were then used, through MLE algorithm, to obtain the unknown value  $N_c$  and estimate the error  $\Delta^2 N_c$ . The theoretical distribution  $p(n|N_c, \eta)$  was obtained by using virtual beam splitter model represented by Eq. (19). In Fig. 3(a) are the numerically obtained errors for probe state  $|3\rangle$  for three different levels of loss, represented by points, compared to quantum FI of the same probe states represented by solid lines. We can see that the errors saturate the CR bound even in the presence of loss and keep the same scaling as the ideal scenario for various  $M$ . In Fig. 3(b) are the same errors plotted with respect to range of losses and compared to optimal Gaussian states with the same mean photon number and without losses, represented by dashed lines, and to vacuum states, represented by dotted lines. We can see that even in the presence of losses, the estimation based on Fock states surpasses even the optimal methods using Gaussian states and optimal coherent measurements. We can also see different trends that appear for the comparison of Fock states to Gaussian and classical limits as the  $N_c$  changes. As  $N_c$  decreases, higher losses can be tolerated before the Fock state estimation falls behind the classical limit, but at the same time lower losses are enough to fall behind methods using optimal Gaussian states. We have observed similar behavior for larger Fock states up to  $m = 7$  from a numerical calculation of Fisher information.

#### IV. SQUEEZING ESTIMATION WITH FOCK STATE PROBE

Let us now turn to the scenario in which we are interested only in the strength of an unknown squeezing operation that can be represented by map  $\mathcal{M}$  in (1) with  $N_c = 0$ . We can analyze this scenario in the same way as the previous

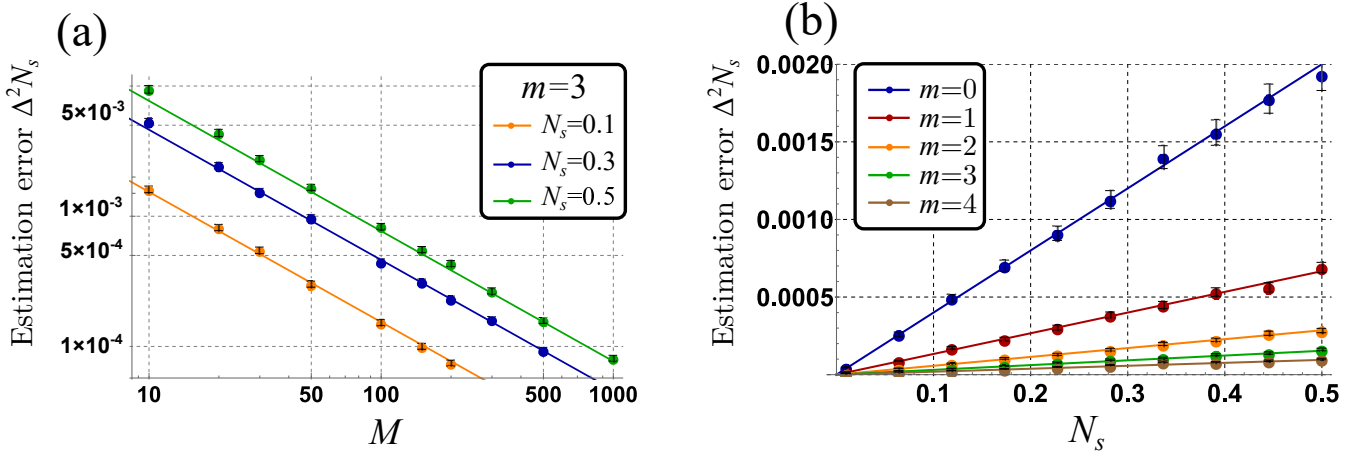


FIG. 4. Simulation for squeezing parameter estimation. The solid lines and circle dots represent the estimation error based on CR bound and simulation averaged over 3000 trials using MLE with the full number statistics  $p(n|N_s)$ . (a) Against the number of copies  $M$  for  $N_s = 0.1, 0.3, 0.5$ . (b) Against the energy added by squeezing  $N_s$  for  $m = 0, 1, 2, 3, 4$ . The number of copies for simulation is  $M = 500$ .

one. After this phase-insensitive squeezing operation, a Fock state  $|m\rangle$  transforms to a mixed state

$$\hat{\rho}_f(N_s) = \int_0^{2\pi} \frac{d\phi}{2\pi} \hat{S}(\sqrt{N_s}e^{i\phi})|m\rangle\langle m|\hat{S}^\dagger(\sqrt{N_s}e^{i\phi}) = \sum_{n=0}^{\infty} p(n|N_s)|n\rangle\langle n|, \quad (21)$$

where [36]

$$p(n|N_s) = |\langle n|\hat{S}(\sqrt{N_s})|m\rangle|^2 = \frac{n!m!}{2^{n-m}} \frac{\tanh^{n-m} \sqrt{N_s}}{\cosh^{2m+1} \sqrt{N_s}} S(\sqrt{N_s}, m, n) \quad \text{when } |m-n| \text{ is even} \quad (22)$$

$$= 0 \quad \text{when } |m-n| \text{ is odd}, \quad (23)$$

with

$$S(r, m, n) = \left| \sum_k \frac{(-1)^k \sinh^{2k} r}{2^{2k} k! (m-2k)! [k + (n-m)/2]!} \right|. \quad (24)$$

Here, the sum is taken for integers  $m$  for which the argument of the factorials is positive. For input Fock states we can explicitly calculate the quantum FI, which is again equal to classical FI for measurement in Fock state basis,

$$F(N_s) = \frac{m^2 + m + 1}{2N_s}. \quad (25)$$

The derivation is similar to that of displacement estimation and is supplied in Appendix A. We can thus analyze the estimation errors again in realistic scenario by numerical simulation. Similar to the displacement estimation case, as the strength of the signal  $N_s$  decreases, the estimation error by ML estimator of (10) saturates the QCR bound for any number of  $M$  as shown in (13).

In Fig. 4(a) and (b), these numerically obtained errors, marked by dots, are shown relative to the number of copies  $M$  and value of the measured squeezing  $N_s$ , respectively. They are again compared to quantum FI represented by solid lines. In both cases we can see that the estimation with Fock states and PNRD again approaches the precision predicted by the CR bound for a broad range of parameters. Increasing the photon number  $m$  of the Fock state probe leads to better performance for the estimation of the phase-insensitive squeezing operation.

Again we can compare the performance of Fock states to the Gaussian methods. When the Gaussian methods cannot take advantage of stable phase, the Gaussian probes can be expressed as mixtures of Fock states and therefore exhibit inferior performance. Numerical tests have confirmed that, in contrast to the displacement estimation, phase randomized squeezed states with arbitrary energy always perform worse than the vacuum state. To see the limits of the Fock-state-based estimation, we compare them to the optimal Gaussian estimation that takes advantage of phase reference. Here, in contrast to the displacement, a pre-displacement of the probe improves the estimation contrast

while increasing mean photon number of the state of the probe. However, our numerical simulations revealed that the improvement gained by this displacement is, with regards to the number of photons added, smaller than what would be gained by additional squeezing with the same number of added photons. We therefore compared the estimation error obtained by Fock states with the FI of Gaussian probes of coherent states or squeezed vacuum states without loss to obtain a strict threshold. Fig. 5 shows the mean photon number of (a) squeezed or (b) coherent states that have the same estimation error as the inverse of the classical FI exhibited by various Fock states and PNRD. The comparison shows that the Fock states are more energy-efficient than the Gaussian states in most cases. This is not the case for estimation of squeezing for small values of  $N_s$  and small  $m$ . It should be noted that in optical sensing, Gaussian states are generally easier to prepare than Fock states, but the difficulty varies wildly. Coherent states can be prepared routinely and are significantly more feasible than impure squeezed states. Preparing completely pure squeezed states, on the other hand, has difficulties comparable to preparation of Fock states. Comparison of equal mean photon numbers in Fig. 5 shows that to attain the same precision with Gaussian states, significantly higher energy is required, which might be an issue for some applications [40]. It is worthwhile to emphasize that our numerical calculation of quantum FI of Gaussian states showed by fitting with respect to the mean photon number that the scaling of quantum FI of coherent state and squeezed state is linear and quadratic with the mean photon number of the probe.

The bounds for coherent and squeezed states can now help us in evaluating the performance of the estimation with Fock states under losses. The first important observation is that there is no simple relation in the estimation of squeezing between the effect of losses before and after the sample. This is because squeezing can lead to entanglement between the probe and the after-sample-bath, which then alters the properties of the probes. However, in the limit of low values of estimated parameter  $N_s \ll 1$ , the effect of squeezing is linearized and this difference can be neglected. In this regime, losses after the channel would alter the estimated value, but the qualitative behavior of the error rates would remain the same. Since this is the regime we are most often interested in, we can again, for the sake of simplicity of analysis, consider only the case with losses before the channel.

We again performed numerical simulation for the estimation errors of squeezing under loss, which are shown in Fig. 6 (a) relative to number of copies  $M$  and (b) relative to the loss rate  $1 - \eta$ . Both figures show that, similarly to the scenario of displacement estimation, the estimation errors under loss approach the CR bound and that the scaling with  $M$  remains consistent. While for small values of  $N_s$  and  $m$  the Fock states and squeezed states with optimal coherent detection are comparable such as  $N_s = 0.1$  and  $m = 3$ , the Fock states enable attaining a better scaling of precision for large  $N_s$  and  $m$  as suggested by Fig. 5 (b) and Fig. 6 (b) for small  $1 - \eta$ .

## V. SIMULTANEOUS ESTIMATION OF DISPLACEMENT AND SQUEEZING

Finally, let us consider a general scenario in which both quantities,  $N_c$  and  $N_s$ , appear at the same time and are estimated simultaneously. This can be part of characterization of a general Gaussian process. Another way this scenario can arise is when squeezing, the nonlinear process we want to characterize, is accompanied by noise with Poissonian distribution that can not be separated from the process. In this scenario we need to attempt simultaneous estimation of both quantities even though we are only ultimately interested in one.

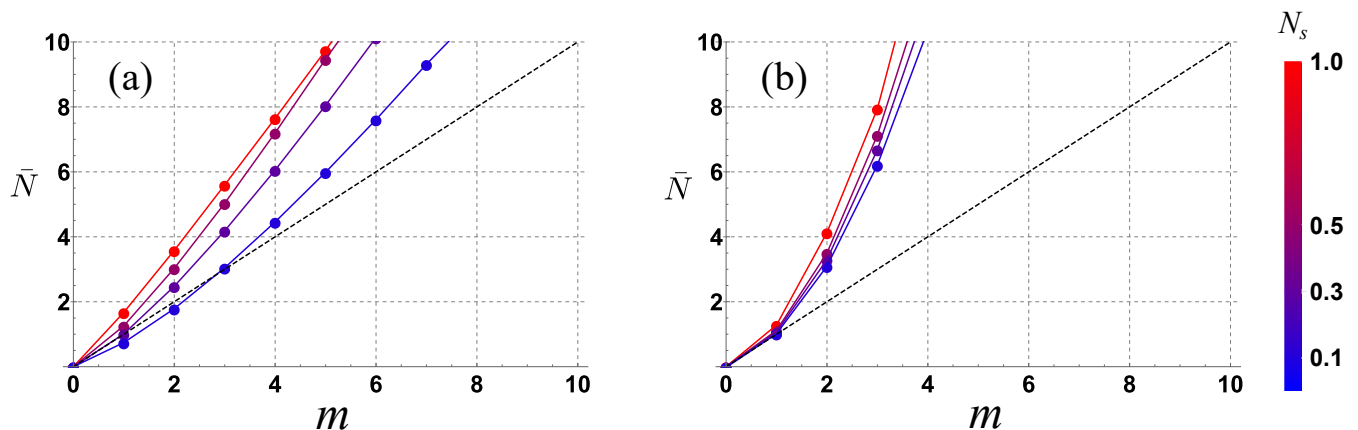


FIG. 5. Average photons required to attain the same quantum FI as classical FI of Fock states with PNRD (a) using squeezed states, (b) using coherent states. The left (right) plot shows that in overall, squeezed (coherent) states require more photon numbers than Fock states.



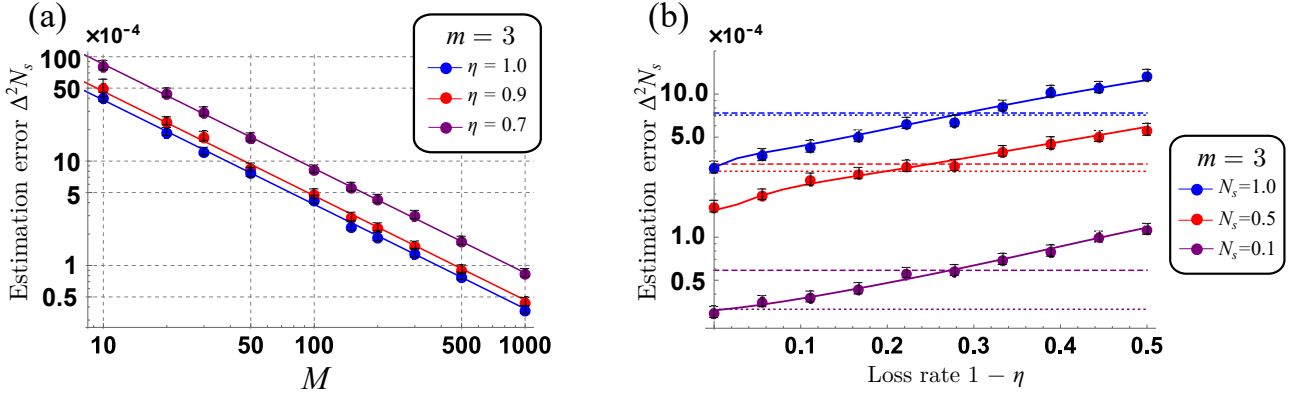


FIG. 6. Simulation for squeezing estimation with a Fock state  $|m = 3\rangle$  as an input probe in the presence of photon-loss. The dots represent the estimation error based on simulation using MLE with the full number statistics  $p(n|N_s)$ , which are obtained by averaging over 1000 trials with  $N_s = 0.25$ . (a) Against the number of copies  $M$ . Similarly to displacement estimation, the CR bound is saturated by MLE for a wide range of  $M$  in the presence of photon-loss. (b) Against loss rate  $1 - \eta$ . The dotted and dashed lines represent the estimation error limit of squeezed states and of coherent states without photon-loss, respectively. These classical estimation limits were evaluated as inverse of quantum FI for the states. The figure clearly showcases several scenarios in which Fock states subjected to loss provide better precision than pure Gaussian states.

After the general channel (1), the Fock state probe will be transformed to

$$\hat{\rho}_f(N_c, N_s) = \mathcal{M}(\hat{\rho}_{in}) = \sum_{n,k=0}^{\infty} w(n|k) q(k|m) |n\rangle \langle n| = \sum_{n=0}^{\infty} p(n|m) |n\rangle \langle n|, \quad (26)$$

where  $q(k|m) = |\langle k|\hat{S}(r)|m\rangle|^2$ ,  $w(n|k) = |\langle n|\hat{D}(\alpha)|k\rangle|^2$ , and  $p(n|m) = \sum_{k=0}^{\infty} w(n|k) q(k|m)$ . The lower bound of error on simultaneous estimation of  $N_c$  and  $N_s$ , or multiparameter CR bound, is given by the quantum FI matrix  $C \geq H^{-1}$  [27, 37–39] with covariance matrix  $C_{N_c, N_c} = \langle (N_c^{\text{est}} - N_c)^2 \rangle$ ,  $C_{N_s, N_s} = \langle (N_s^{\text{est}} - N_s)^2 \rangle$ ,  $C_{N_c, N_s} = C_{N_s, N_c} = \langle (N_c^{\text{est}} - N_c)(N_s^{\text{est}} - N_s) \rangle$ . Here the matrix inequality  $A \geq B$  means that  $A - B$  is a positive semi-definite matrix. Since the final state is always diagonal in the Fock basis, the quantum FI matrix, which is the same as the classical FI matrix based on the PNRD, can be written as

$$H(N_c, N_s) = \begin{pmatrix} H_{N_c, N_c} & H_{N_c, N_s} \\ H_{N_s, N_c} & H_{N_s, N_s} \end{pmatrix}, \quad (27)$$

with

$$H_{x,y} = \sum_{n=0}^{\infty} \frac{1}{p(n|m)} \left( \frac{\partial p(n|m)}{\partial x} \right) \left( \frac{\partial p(n|m)}{\partial y} \right), \quad (28)$$

$$(29)$$

where  $x, y$  are in  $\{N_c, N_s\}$ . The classical multiparameter CR bound can also be asymptotically saturated by ML estimator. From the multiparameter CR bound, we can extract the estimation errors of each parameter,

$$\Delta^2 N_c \geq \frac{H_{N_s, N_s}}{H_{N_c, N_c} H_{N_s, N_s} - H_{N_c, N_s}^2} = H_{N_c, N_c}^{-1} (1 - H_{N_c, N_s}^2 / H_{N_c, N_c} H_{N_s, N_s})^{-1}, \quad (30)$$

$$\Delta^2 N_s \geq \frac{H_{N_c, N_c}}{H_{N_c, N_c} H_{N_s, N_s} - H_{N_c, N_s}^2} = H_{N_s, N_s}^{-1} (1 - H_{N_c, N_s}^2 / H_{N_c, N_c} H_{N_s, N_s})^{-1}. \quad (31)$$

When more than one parameter in the process are involved, two main difficulties arise that may degrade the estimation error [27, 41]. First of all, as shown in inequalities (30) and (31), the off-diagonal elements of FI matrix decrease the estimation error for fixed diagonal elements. Non-vanishing off-diagonal elements of FI matrix imply that the parameters interplay each other in the process, so that one needs to know the other parameters in order to estimate a parameter of interest precisely. On the other hand, when the off-diagonal element of the FI matrix vanishes, the estimation errors reduce to

$$\Delta^2 N_c \geq H_{N_c, N_c}^{-1}, \quad (32)$$

$$\Delta^2 N_s \geq H_{N_s, N_s}^{-1}. \quad (33)$$

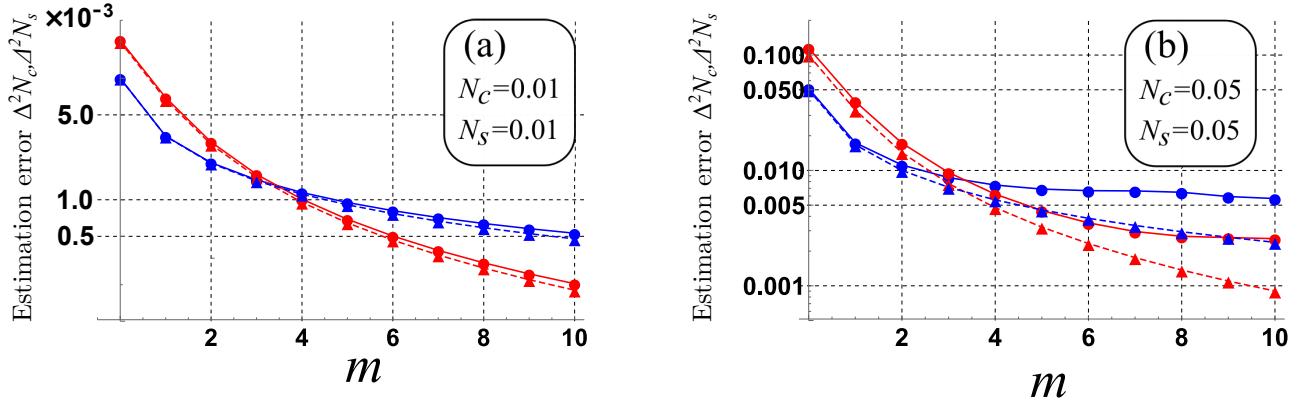


FIG. 7. Simultaneous estimation errors for  $N_c$  (blue lines) and  $N_s$  (red lines). More specifically, solid lines with circles represent the lower bound of the estimation error in Eq. (30) and Eq. (31), respectively. Dashed lines with triangles represent the quantum FI of Fock state probe for estimating  $N_c(N_s)$  when  $N_s(N_c)$  is 0 and known. (a) shows values for estimating  $N_c = N_s = 0.01$ , (b) shows values for estimating  $N_c = N_s = 0.05$ .

Thus, when the off-diagonal element of the FI matrix is much smaller than the diagonal elements, the estimation error of each parameter is bounded by the inverse of each diagonal element of the FI matrix. In this case, we can interpret the inequalities as that of a single-parameter estimation where any information about the other parameters is not required to estimate the parameter of interest.

The second difficulty is that even when one is estimating a single parameter, since the other parameters are involved, the diagonal elements of quantum (classical) FI may decrease. For instance, when we estimate the squeezing parameter  $N_s$ , the displacement process in Map (26), written as  $w(n|k)$ , plays a role of a noisy process in the measurement setup. Similarly when we estimate the displacement parameter  $N_c$ , the squeezing process in Map (26), written as  $q(k|m)$ , plays a role as a preparation error. Thus, generally when more than one parameter is involved, the estimation error may decrease. We investigate our case by numerical simulation focusing on these difficulties.

In Fig. 7(a) and (b), we show the numerically calculated the lower bounds of the estimation errors for two different sets of measured values. We numerically confirmed that the off-diagonal elements are very small compared to the diagonal elements ( $H_{N_c, N_s}^2 / H_{N_c, N_c} H_{N_s, N_s} < 10^{-3}$  in Fig. 7(a) and  $H_{N_c, N_s}^2 / H_{N_c, N_c} H_{N_s, N_s} < 1.2 \times 10^{-2}$  in Fig. 7(b)), which means that we do not suffer from the first difficulty in this regime and that the inverse of the diagonal components of FI matrix approximately give the lower bounds of the estimation errors of each quantity as written in Eqs. (32) and (33). This is best seen for small values of estimated parameters in Fig. 7(a) where the off-diagonal elements are truly negligible and errors are practically identical, whether both quantities are measured or just single ones. In Fig. 7(b), where the estimated parameters are not as small, the quantities start disturbing each other and the deviation from the individual estimations increase. When the estimated parameters are not small enough, the role of the other parameter as a noisy process becomes so dominant that highly nonclassical states such as Fock states of large photon numbers may cease to give a small estimation error as shown in Fig. 7(b).

## VI. CONCLUSION

In this work, we have investigated the possibility of using Fock states and photon number resolving detectors for parameter estimation of single mode Gaussian unitaries in the absence of stable phase reference. This scenario is relevant in optical sensing when stable phase reference is unavailable through the sample, for example because of random nature of the examined operation and the light emitted by the sample is weak.

To accommodate both points of view, we have evaluated the performance of Fock states under realistic environment and compared them to the optimal performance of phase-sensitive Gaussian states with no loss and optimal quantum measurement. We found out that for estimation of both weak displacement and squeezing, the Fock states together with Fock basis detection can, already for ensemble of 500 trials saturate the Cramér-Rao bound and provide error rates surpassing optimal Gaussian states with equivalent mean photon number. Loss incurred in the sample or during preparation of the probes limits the quality of the estimation. The influence generally depends on the strength of the measured interaction. When  $N_c, N_s \approx 0.5$ , Fock states outperform the Gaussian bounds even when affected by 20% losses. When  $N_c, N_s \approx 0.1$ , loss of 20% can be tolerated when compared to coherent states, but less than 5% loss brings the Fock states above the level of pure squeezed states. Simultaneous estimation of both squeezing

and displacement is also possible without being disturbed from each other and it works best in the limit of small parameters,  $N_c, N_S < 0.1$ , when the operations are effectively independent. Together, these features can allow either multi-parameter estimation of an optical Gaussian process in various systems, including atomic physics and solid-state physics, or estimation of new squeezing processes under inherent Poissonian noise. The method can also be extended for estimation of higher order processes which encompass joint  $n$ -photon effects.

Experimental application of the procedure relies on Fock states and measurements in Fock basis. The measurement requires photon number resolving detectors. Transition edge sensors (TES) [42–46] is well known to be promising in this area as they are already capable of resolving up to 12 photons with estimated 0.98 detection efficiency [47]. Alternatively, detector with photon number resolving capability can be constructed from an array of on-off detectors [48–54], or it can be, for purposes of proof-of-concept tests, replaced altogether by homodyne tomography. The photon number resolving detectors can be also used for preparation of the Fock states for the probes. Detecting a specific Fock state in one mode of a two-mode squeezed state generated by Optical Parametric Oscillator (OPO) projects the other mode into the same Fock state and is a technique often employed in quantum optics. It is also possible to generate the necessary Fock states by merging single photon states [55], which can be generated by quantum dots [56–60]. A proof-of-principle experimental test of the estimation method could be immediately realized with Fock states  $|1\rangle$  or  $|2\rangle$ , conditionally obtained from an OPO, measured by TES and homodyne tomography for the verification purposes. Finally, the detection method can be also considered outside the area of quantum optics. For example, experiments with trapped ions are well suited both for preparation of Fock states and estimating their altered Fock state distribution [10, 25].

## VII. ACKNOWLEDGEMENT

We acknowledge project 19-19722J of the Grant Agency of Czech Republic (GAČR). C. O. acknowledge support from NSF (OMA-1936118). K. P. acknowledges Danish National Research Foundation through the Center of Excellence for Macroscopic Quantum States (bigQ, DNRF142). R. F. also acknowledges the MEYS of the Czech Republic (grant agreements 02.1.01/0.0/0.0/16\_026/0008460 and 8C20002) and the funding from European Union's Horizon 2020 (2014-2020) research and innovation framework programme under grant agreement No 731473 (ShoQC). Project ShoQC has received funding from the QuantERA ERA-NET Cofund in Quantum Technologies implemented within the European Union's Horizon 2020 Programme. H. J. acknowledges the National Research Foundation of Korea through grants funded by the Korea Government (NRF-2019M3E4A1080074 and NRF-2020R1A2C1008609).

## APPENDIX A: QUANTUM FISHER INFORMATION

Let us consider a unitary operation  $\hat{U} = e^{-i\hat{H}\theta}$  where the Hamiltonian  $\hat{H}$  generates  $\theta$ . In the case of displacement,  $\hat{H} = \hat{a} + \hat{a}^\dagger$ , and for squeezing,  $\hat{H} = i(\hat{a}^2 - \hat{a}^{\dagger 2})$ . After the phase-randomized displacement or squeezing operation, the output state can be written as

$$\hat{\rho}_f = \sum_{n=0}^{\infty} p(n|m) |n\rangle\langle n| = \sum_{n=0}^{\infty} |\langle n|\hat{U}|m\rangle|^2 |n\rangle\langle n|. \quad (\text{A1})$$

Let us first consider displacement estimation,  $\hat{U} = e^{\alpha\hat{a}^\dagger - \alpha^*\hat{a}}$ . Since the final state is diagonal in Fock basis, the derivation of classical Fisher information of  $p(n|m)$  is sufficient. The classical Fisher information for  $|\alpha|$  is written as

$$F(|\alpha|) = \sum_{n=0}^{\infty} \frac{1}{p(n|m)} \left( \frac{\partial p(n|m)}{\partial |\alpha|} \right)^2. \quad (\text{A2})$$

Assuming  $\alpha$  to be real without loss of generality, the differential term is simplified as

$$\left( \frac{\partial p(n|m)}{\partial |\alpha|} \right)^2 = \left( -\langle n|\hat{D}(\alpha)|m\rangle\langle m|\hat{D}^\dagger(\alpha)(\hat{a}^\dagger - \hat{a})|n\rangle + \langle n|\hat{D}(\alpha)(\hat{a}^\dagger - \hat{a})|m\rangle\langle m|\hat{D}^\dagger(\alpha)|n\rangle \right)^2 \quad (\text{A3})$$

$$= \left( \langle n|\hat{D}(\alpha)|m\rangle\langle m|\hat{D}^\dagger(\alpha)(\hat{a}^\dagger - \hat{a})|n\rangle \right)^2 + \left( \langle n|\hat{D}(\alpha)(\hat{a}^\dagger - \hat{a})|m\rangle\langle m|\hat{D}^\dagger(\alpha)|n\rangle \right)^2 \\ - 2\langle n|\hat{D}(\alpha)|m\rangle\langle m|\hat{D}^\dagger(\alpha)(\hat{a}^\dagger - \hat{a})|n\rangle\langle n|\hat{D}(\alpha)(\hat{a}^\dagger - \hat{a})|m\rangle\langle m|\hat{D}^\dagger(\alpha)|n\rangle \quad (\text{A4})$$

$$= 4p(n|m)\langle m|\hat{D}^\dagger(\alpha)(\hat{a}^\dagger - \hat{a})|n\rangle\langle n|\hat{D}(\alpha)(\hat{a} - \hat{a}^\dagger)|m\rangle. \quad (\text{A5})$$

Finally, we obtain the Fisher information

$$F(|\alpha\rangle) = 4\langle m|\hat{D}^\dagger(\alpha)(\hat{a}^\dagger - \hat{a})\hat{D}(\alpha)(\hat{a} - \hat{a}^\dagger)|m\rangle = 4\langle m|(\hat{a}^\dagger - \hat{a})(\hat{a} - \hat{a}^\dagger)|m\rangle = 8m + 4. \quad (\text{A6})$$

Simiarly, one can check that  $F(r) = 2(m^2 + m + 1)$ .

Since we are interested in the Fisher information about  $N_c = |\alpha|^2$ , one can use the chain-rule for the classical Fisher information such as,

$$F(N_c) = \sum_{n=0}^{\infty} \frac{1}{p(n|m)} \left( \frac{\partial p(n|m)}{\partial N_c} \right)^2 = \frac{1}{4N_c} \sum_{n=0}^{\infty} \frac{1}{p(n|m)} \left( \frac{\partial p(n|m)}{\partial |\alpha|} \right)^2 = \frac{F(|\alpha|)}{4N_c} = \frac{2m+1}{N_c}. \quad (\text{A7})$$

Similarly, the Fisher information about  $N_s = r^2$  is obtained by

$$F(N_s) = \sum_{n=0}^{\infty} \frac{1}{p(n|m)} \left( \frac{\partial p(n|m)}{\partial N_s} \right)^2 = \frac{1}{4N_s} \sum_{n=0}^{\infty} \frac{1}{p(n|m)} \left( \frac{\partial p(n|m)}{\partial r} \right)^2 = \frac{F(r)}{4N_s} = \frac{m^2 + m + 1}{2N_s}. \quad (\text{A8})$$

## APPENDIX B: ESTIMATING DISPLACEMENT BY MEAN INTENSITY MEASUREMENT

When we are able to measure average energy of the probe but not the exact Fock state distribution we can only use the averaged moments

$$\langle \hat{n} \rangle = m + N_c \quad (\text{B1})$$

$$\langle \hat{n}^2 \rangle = m^2 + 2N_c(2m+1) + N_c^2 \quad (\text{B2})$$

$$\Delta^2 \hat{n} = \langle \hat{n}^2 \rangle - \langle \hat{n} \rangle^2 = 2N_c(m+1). \quad (\text{B3})$$

The signal-to-noise ratio (SNR) can be defined where the signal is the change in the average photon number of the probe and the noise is the uncertainty in the photon number as

$$\text{SNR} = \frac{\langle \hat{n} \rangle - m}{\sqrt{\Delta^2 \hat{n}}} = \sqrt{\frac{N_c}{2(m+1)}}. \quad (\text{B4})$$

Here, we notice that SNR has completely inverse tendencies from the Fisher information against  $m$  and  $N_c$ , i.e. a larger precision for a small  $m$  and a large  $N_c$ . The linearized sensitivity  $(\Delta^2 N_c)_{\hat{O}} = \Delta^2 \hat{O} / |\partial \langle \hat{O} \rangle / \partial N_c|^2$  based on  $\langle \hat{n} \rangle$  gives an information about the uncertainty of  $N_c$  by measuring the observable  $\hat{O}$  which is given as

$$(\Delta^2 N_c)_{\hat{n}} = \frac{\Delta^2 \hat{n}}{(\partial \langle \hat{n} \rangle / \partial N_c)^2} = 2N_c(m+1). \quad (\text{B5})$$

Similarly, we can test the linearized sensitivity based on the second moment,

$$\langle \hat{n}^4 \rangle - \langle \hat{n}^2 \rangle^2 = 2(4m+1)N_c^3 + (18m^2 + 2m + 3)N_c^2 + (8m^3 + 2m^2 + 6m + 1)N_c \simeq 8m^3 N_c, \quad (\text{B6})$$

$$\frac{\langle \hat{n}^4 \rangle - \langle \hat{n}^2 \rangle^2}{(\partial \langle \hat{n}^2 \rangle / \partial N_c)^2} \simeq \frac{1}{2}mN_c, \quad (\text{B7})$$

where the approximation is under the condition of a small  $N_c$  and a large  $m$ . It shows that the error based on the second moment also increases with  $m$ . Note that a high linearized sensitivity indicates a less precise measurement, or a large error. The error increases with  $m$  and the best probe is the vacuum probe, and therefore the Fock state probes do not give any advantage. Therefore, we know that the gain in Fisher information of Eq. (16) cannot be obtained by simply using the information about average photon number  $\langle \hat{n} \rangle$ . These results imply that the information about mean values does not provide the scalings of sensitivity available by estimation strategies with PNRD.

---

[1] V. Giovannetti, S. Lloyd, and L. Maccone, Quantum-Enhanced Measurements: Beating the Standard Quantum Limit, Science **306**, 1330 (2004).

- [2] V. Giovannetti, S. Lloyd, and L. Maccone, Quantum metrology. *Phys. Rev. Lett.* **96**, 010401 (2006).
- [3] V. Giovannetti, S. Lloyd, and L. Maccone, Advances in quantum metrology, *Nat. Photon.* **5**, 222-229 (2011).
- [4] S. Pirandola et al., Advances in photonic quantum sensing, *Nat. Phot.* **12**, 724 (2018).
- [5] R. Demkowicz-Dobrzanski, M. Jarzyna, and J. Koodyski. Quantum limits in optical interferometry. *Progress in Optics* 2015 Jan 1 (Vol. 60, pp. 345-435). Elsevier.
- [6] C. M. Caves, Quantum-mechanical noise in an interferometer, *Phys. Rev. D* **23**, 1693 (1981).
- [7] S. Olivares, M. G. A. Paris, Bayesian estimation in homodyne interferometry, *J. Phys. B* **42**, 055506 (2009).
- [8] A. A. Berni et al., Ab initio quantum-enhanced optical phase estimation using real-time feedback control, *Nat. Photon.* **9**, 577 (2015).
- [9] C. Oh et al., Optimal Gaussian measurements for phase estimation in single-mode Gaussian metrology, *npj Quantum Information* **5**, 10 (2019).
- [10] K. C. McCormick et al. Quantum-enhanced sensing of a single-ion mechanical oscillator. *Nature* **572**, 7767 (2019).
- [11] H. Lee, P. Kok, and J. P. Dowling, A quantum Rosetta stone for interferometry. *J. Mod. Opt.* **49**, 2325 (2002).
- [12] J. P. Dowling, Quantum optical metrology the lowdown on high-N00N states, *Contemp. Phys.* **49**, 125 (2008).
- [13] W. P. Schleich, *Quantum optics in phase space*. John Wiley & Sons (2011).
- [14] M. G. Genoni, M. G. A. Paris, G. Adesso, H. Nha, P. L. Knight, and M. S. Kim, Optimal estimation of joint parameters in phase space, *Phys. Rev. A* **87**, 012107 (2013).
- [15] W. H. Zurek, Sub-Planck structure in phase space and its relevance for quantum decoherence, *Nature (London)* **412**, 712 (2001).
- [16] K. Duivenvoorden, B. M. Terhal, D. Weigand, Single-Mode Displacement Sensor, *Phys. Rev. A* **95**, 012305 (2017).
- [17] O. Pinel, P. Jian, N. Treps, C. Fabre, and D. Braun, Quantum parameter estimation using general single-mode Gaussian states, *Phys. Rev. A* **88**, 040102 (R) (2013).
- [18] D. afrneek, A. R. Lee and I. Fuentes, Quantum parameter estimation using multi-mode Gaussian states, *New. J. Phys.* **17**, 073016 (2015).
- [19] D. afrneek and I. Fuentes, Optimal probe states for the estimation of Gaussian unitary channels, *Phys. Rev. A* **94**, 062313 (2016).
- [20] R. Nichols, P. Liuzzo-Scorpo, P. A. Knott, and G. Adesso, Multiparameter Gaussian quantum metrology, *Phys. Rev. A* **98**, 012114 (2018).
- [21] D. afrneek, Estimation of Gaussian quantum states, *J. Phys. A* **52**, 035304 (2019).
- [22] C. Oh, C. Lee, L. Banchi, S.-Y. Lee, C. Rockstuhl, and H. Jeong, Optimal measurements for quantum fidelity between Gaussian states and its relevance to quantum metrology, *Phys. Rev. A* **100**, 012323 (2019).
- [23] B. M. Escher, R. L. de Matos Filho and L. Davidovich, General framework for estimating the ultimate precision limit in noisy quantum-enhanced metrology, *Nat. Phys.* **7**, 406 (2011).
- [24] S. Slussarenko et al. Unconditional violation of the shot-noise limit in photonic quantum metrology, *Nature Photonics* 11.11 (2017): 700-703.
- [25] F. Wolf et al., Motional Fock states for quantum-enhanced amplitude and phase measurements with trapped ions, *Nature comm.* **10**, 1 (2019).
- [26] G. Chiribella, G. M. D'Ariano and M. F. Sacchi, Joint estimation of real squeezing and displacement, *J. Phys. A* **39**, 2127 (2006).
- [27] C. W. Helstrom, *Quantum Detection and Estimation Theory* (Academic Press, New York, 1976).
- [28] S. L. Braunstein and C. M. Caves, Statistical Distance and the Geometry of Quantum States, *Phys. Rev. Lett.* **72**, 3439 (1994).
- [29] R. A. Fisher, Theory of Statistical Estimation, *Proc. Camb. Soc.* **22**, 700 (1925).
- [30] S. L. Braunstein, How large a sample is needed for the maximum likelihood estimator to be approximately Gaussian?, *J. Phys. A* **25**, 3813 (1992).
- [31] S. L. Braunstein, Quantum limits on precision measurements of phase, *Phys. Rev. Lett.* **69**, 3598 (1992).
- [32] M. G. A. Paris, Quantum estimation for quantum technology. *International Journal of Quantum Information*, *Int. J. Quant. Inf.* **7**, 125 (2009).
- [33] F. A. M. de Oliveira, M. S. Kim, and P. L. Knight, V. Buick, Properties of displaced number states, *Phys. Rev. A* **41**, 2645 (1990).
- [34] C. Schäfermeier, M. Ježek, L. S. Madsen, T. Gehring, U. L. Andersen, Deterministic phase measurements exhibiting super-sensitivity and super-resolution, *Optica* **5**, 60 (2018)
- [35] D. F. Walls, and G. J. Milburn, 1995, Eds., *Quantum Optics* (Springer, Berlin).
- [36] M. S. Kim, F. A. M. de Oliveira, and P. L. Knight, Properties of squeezed number states and squeezed thermal states, *Phys. Rev. A* **40**, 2494 (1989).
- [37] M. Szczykulska, T. Baumgratz, and A. Datta, Multi-parameter quantum metrology, *Adv. Phys.: X* **1**, 621 (2016).
- [38] M. Gessner, L. Pezz, and A. Smerzi, Sensitivity Bounds for Multiparameter Quantum Metrology, *Phys. Rev. Lett.* **121**, 130503 (2018)
- [39] J. Liu, H. Yuan, X.-M. Lu, and X. Wang, Quantum Fisher information matrix and multiparameter estimation, *J. Phys. A: Math. Theor.* **53**, 023001 (2020).
- [40] Michael A. Taylor, Warwick P. Bowen, Quantum metrology and its application in biology, *Physics Reports* 615, 1-59 (2016).
- [41] T. J. Proctor, P. A. Knott, and J. A. Dunningham. Multiparameter estimation in networked quantum sensors. *Phys. Rev. Lett.* **120**, 080501 (2018)

- [42] A. E. Lita, A. J. Miller, and S. W. Nam, Counting near-infrared single-photons with 95% efficiency, *Optics Express* **16**, 3032 (2008).
- [43] B. Calkins, P. L. Mennea, A. E. Lita, B. J. Metcalf, W. S. Kolthammer, A. Lamas-Linares, J. B. Spring, P. C. Humphreys, R. P. Mirin, J. C. Gates, P. G. R. Smith, I. A. Walmsley, T. Gerrits, and S. W. Nam, High quantum-efficiency photon-number-resolving detector for photonic on-chip information processing, *Opt. Express* **21**, 22657–22670 (2013).
- [44] F. Marsili, V. B. Verma, J. A. Stern, S. Harrington, A. E. Lita, T. Gerrits, I. Vayshenker, B. Baek, M. D. Shaw, R. P. Mirin, and S. W. Nam, Detecting single infrared photons with 93% system efficiency, *Nature Photonics* **7**, 210 (2013).
- [45] G. Harder, T. J. Bartley, A. E. Lita, S. W. Nam, T. Gerrits, and C. Silberhorn, Single-mode parametric-down-conversion states with 50 photons as a source for mesoscopic quantum optics, *Phys. Rev. Lett.* **116**, 143601 (2016).
- [46] I. A. Burenkov, A. K. Sharma, T. Gerrits, G. Harder, T. J. Bartley, C. Silberhorn, E. A. Goldschmidt, and S. V. Polyakov, Full statistical mode reconstruction of a light field via a photon-number-resolved measurement, *Phys. Rev. A* **95**, 053806 (2017).
- [47] J. Sperling, W. R. Clements, A. Eckstein, M. Moore, J. J. Renema, W. S. Kolthammer, S. W. Nam, A. Lita, T. Gerrits, W. Vogel, G. S. Agarwal, and I. A. Walmsley, Detector-independent verification of quantum light, *Phys. Rev. Lett.* **118**, 163602 (2017).
- [48] D. Achilles, C. Silberhorn, and I. A. Walmsley, Direct, loss-tolerant characterization of nonclassical photon statistics, *Phys. Rev. Lett.* **97**, 043602 (2006).
- [49] M. Avenhaus, H. B. Coldenstrodt-Ronge, K. Laiho, W. Mauerner, I. A. Walmsley, and C. Silberhorn, Photon number statistics of multimode parametric down-conversion, *Phys. Rev. Lett.* **101**, 053601 (2008).
- [50] M. A. Usuga, C. R. Müller, C. Wittmann, P. Marek, R. Filip, C. Marquardt, G. Leuchs, and U. L. Andersen, Noise-powered probabilistic concentration of phase information, *Nature Physics* **6**, 767 (2010).
- [51] M. Yukawa, K. Miyata, T. Mizuta, H. Yonezawa, P. Marek, R. Filip, and A. Furusawa, Generating superposition of up-to three photons for continuous variable quantum information processing, *Opt. Express* **21**, 5529–5535 (2013).
- [52] G. Harder, C. Silberhorn, J. Rehacek, Z. Hradil, L. Motka, B. Stoklasa, and L. L. Sánchez-Soto, Local sampling of the wigner function at telecom wavelength with loss-tolerant detection of photon statistics, *Phys. Rev. Lett.* **116**, 133601 (2016).
- [53] M. Bohmann, J. Tiedau, T. Bartley, J. Sperling, C. Silberhorn, and W. Vogel, Incomplete detection of nonclassical phase-space distributions, *Phys. Rev. Lett.* **120**, 063607 (2018).
- [54] M. Cooper, L. J. Wright, C. Soller, and B. J. Smith, Experimental generation of multi-photon Fock states, *Optics Express* **21**, 5309 (2013).
- [55] K. R. Motes, R. L. Mann, J. P. Olson, N. M. Studer, E. A. Bergeron, A. Gilchrist, J. P. Dowling, D. W. Berry, and P. P. Rohde Efficient recycling strategies for preparing large Fock states from single-photon sources: Applications to quantum metrology *Phys. Rev. A* **94**, 012344 (2016).
- [56] G. Bulgarini, M. E. Reimer, M. B. Bavinck, K. D. Jöns, D. Dalacu, P. J. Poole, E. P. A. M. Bakkers, and V. Zwiller, Nanowire Waveguides Launching Single Photons in a Gaussian Mode for Ideal Fiber Coupling, *Nano Lett.* **14**, 4102 (2014).
- [57] X. Ding, Y. He, Z.-C. Duan, N. Gregersen, M.-C. Chen, S. Unsleber, S. Maier, C. Schneider, M. Kamp, S. Höfling, C.-Y. Lu, and J.-W. Pan, On-demand single photons with high extraction efficiency and near-unity indistinguishability from a resonantly driven quantum dot in a micropillar, *Phys. Rev. Lett.* **116**, 020401 (2016).
- [58] P. Senellart, G. Solomon, and A. White, High-performance semiconductor quantum-dot single-photon sources, *Nature nanotechnology* **12**, 1026 (2017).
- [59] L. Dusanowski, S.-H. Kwon, C. Schneider, and S. Höfling, Near-Unity Indistinguishability Single Photon Source for Large-Scale Integrated Quantum Optics, *Phys. Rev. Lett.* **122**, 173602 (2019)
- [60] H. Ollivier, I. M. de Buy Wenniger, S. Thomas, S. C. Wein, A. Harouri, G. Coppola, P. Hilaire, C. Millet, A. Lemaître, I. Sagnes, O. Krebs, L. Lanco, J. C. Loredó, C. Antón, N. Somaschi, and P. Senellart, Reproducibility of High-Performance Quantum Dot Single-Photon Sources, *ACS Photonics* **7**, 1050 (2020)